

Jonathan J. Gourley, Pierre Tabary, and Jacques Parent du Chatelet  
 Météo-France, DSO, Centre de Meteorologie Radar, Trappes, France

1. INTRODUCTION

Molecular absorption by the precipitation media is known to reduce values of horizontal reflectivity ( $Z_H$ ) and differential reflectivity ( $Z_{DR}$ ) for precipitation radars operating at relatively short wavelengths. This attenuation effect is most pronounced behind intense convective echoes. With the advent of polarization diversity, differential propagation phase measurements ( $\Phi_{DP}$ ) offer the advantages of being immune to radar calibration errors, attenuation effects, hail contamination, and partial beam blocking (Ryzhkov and Zrnic 1995). Moreover, Holt (1988) and Bringi et al. (1990) discovered that coefficients used to correct both  $Z_H$  and  $Z_{DR}$  were linearly related to  $\Phi_{DP}$  measurements. Fig. 1 shows actual observations of  $Z_{DR}$  and  $\Phi_{DP}$ . It is evident that low values of  $Z_{DR}$  are coincident with high values of  $\Phi_{DP}$ . Several methods have emerged which utilize  $\Phi_{DP}$  as a basis to correct for the reduction in  $Z_H$  and  $Z_{DR}$  due to attenuation. This paper demonstrates a new methodology, called the advection-correction technique, that is independent of an assumed raindrop size-shape model, b) may accommodate temperature-dependent attenuation, and c) is semi-empirical.

The technique presented here essentially tracks echoes from one image to the next and then assumes that any changes in  $Z_H$  and  $Z_{DR}$  are due to attenuation effects alone. Correction factors based on  $\Phi_{DP}$  measurements are produced for several cases of intense convection. Comparisons of corrected versus uncorrected reflectivity measurements are made using data collected at neighboring radars.

2. ADVECTION-CORRECTION TECHNIQUE

The technique is based on the assumption that, in the mean, changes in  $Z_H$  and  $Z_{DR}$  over a 5-min period are due to attenuation effects alone. First, a cross-correlation analysis is used to derive propagation vectors and advect the echoes in order to account for their movement between subsequent images (see Figs. 1 and 2). Modeled values of  $Z_H$ ,  $Z_{DR}$ , and  $\Phi_{DP}$  are grouped with observations of all three fields valid 5-min later. For example, in Fig. 1 we see that an increase in  $Z_{DR}$  at a given grid point is associated with a decrease in  $\Phi_{DP}$ . Such analyses are performed at each grid point for several hours in which there is intense convection. The observed and modeled values are stored to file and are used to calculate the 2-way, total attenuation and differential attenuation vectors,  $A_h(\Phi_{DP})$  and  $A_{hv}(\Phi_{DP})$ .

\* Corresponding author address: Jonathan J. Gourley, Centre de Meteorologie Radar, DSO, Météo France, 7 rue Teisserenc-de-Bort 78195, Trappes, France; email: jonathan.gourley@meteo.fr

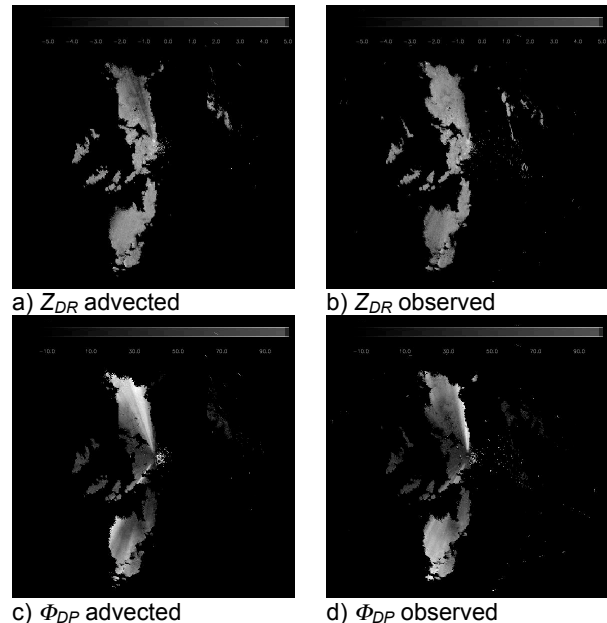


**FIG. 1.** Images collected from the Trappes polarimetric radar which show a negative correlation between  $Z_{DR}$  and  $\Phi_{DP}$ .

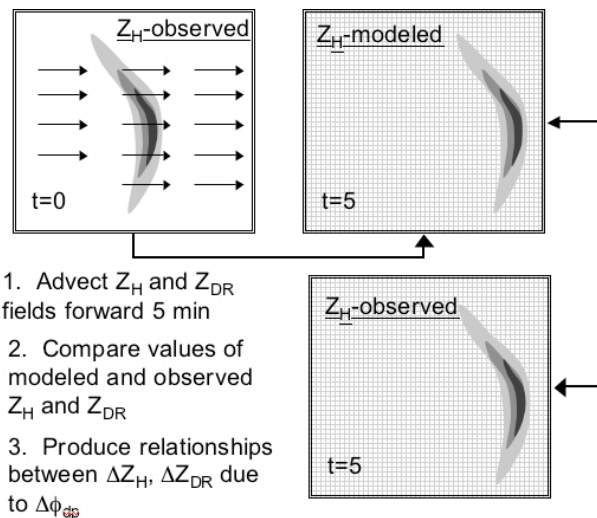


**FIG. 2.** Illustration of the advection-correction scheme. At the initial time, advection vectors are used to march the  $Z_H$  and  $Z_{DR}$  fields forward 5 min. The advected fields are then compared with observations valid at the same time. Differences are attributed to attenuation and are coupled with  $\Phi_{DP}$  differences.

For simplicity, the correction to  $Z_H$  is demonstrated here, bearing in mind that the same analysis is performed for  $Z_{DR}$ . First, we assume that any change in the value of  $Z_H$  advected 5-min into the future may only be attributed to nonzero attenuation effects:

$$Z_i^{obs}(i) - Z_i^{adv}(i) = \bar{A}_h(\Phi_{DP}^{obs}(i) - \Phi_{DP}^{adv}(i)); i = 1 \dots nmsmts, \quad (1)$$

This assumption may not hold for cells that are either growing or decaying, but it does hold in a mean sense. In order to mitigate storm lifecycle effects, we have limited our dataset to  $Z_H < 40$  dBZ,  $\rho_{HV}(0) > 0.97$  to improve the quality of the data, and altitude  $< 3.0$  km to remain below the melting layer. In addition, the values of  $\Phi_{DP}$  in Eq. (1) must be different by at least  $30^\circ$ . Eq. (1) is rewritten in matrix form, and the system is over-determined given the large number of measurements available at each grid point between successive images. A solution is then sought out in a least square form by introducing a cost function and minimizing. The attenuation vector,  $A_h$ , is solved for and provides a basis for correcting  $Z_H$  measurements given values of  $\Phi_{DP}$ . Two constraints were employed to make the retrievals well-posed.  $A_h(0)$  is forced to 0 dB, and the slope of the  $A_h(\Phi_{DP})$  line is used, thus linearity is assumed.

Six convective events that occurred during spring of 2005 are used to retrieve  $A_h(\Phi_{DP})$  and  $A_{hv}(\Phi_{DP})$ . Fig. 3 shows the resulting curves that subsequently may be used to correct  $Z_H$  and  $Z_{DR}$ . The gray lines refer to the reported ranges of correction coefficients for data collected at C-band as summarized in Carey et al. (2000). The larger coefficients are those that correspond to large drops ( $D_o > 2.5$  mm). The retrieved values fall within the bounds found by other investigators. Additional sensitivity tests will be performed in the future in order to understand the variability of the  $A_h$  and  $A_{hv}$  retrievals from case-to-case.

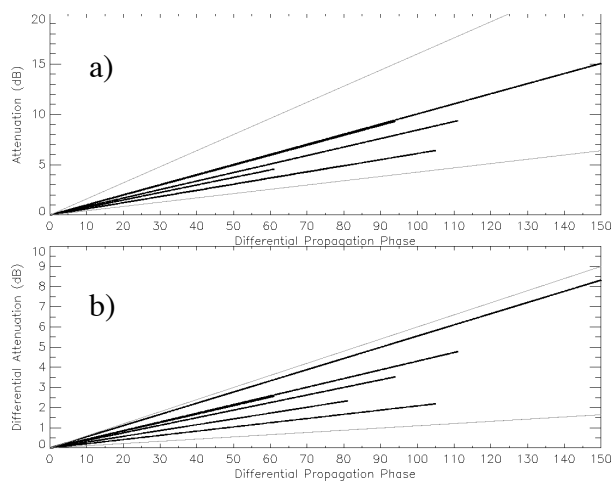


**FIG. 3.** Plot of retrieved values of a) total horizontal attenuation and b) total differential attenuation as a function of  $\Phi_{DP}$ . Thin gray lines correspond to expected ranges as reported in Carey et al. (2000).

### 3. RADAR-RADAR $Z_H$ COMPARISONS

#### a. No attenuation correction

The Trappes C-band polarimetric radar is located approximately 30 km southwest of Paris, France. There are three, non-polarimetric radars in the vicinity (Abbeville, Bourges, and Falaise) that operate continuously as part of the French radar network. These radars are used to evaluate the effectiveness of  $A_h$  retrievals from the advection-correction scheme. A similar approach could be implemented for evaluating  $A_{hv}$  retrievals provided there are neighboring polarimetric radars. Radar reflectivity comparisons are performed on as much as 24 hours of data on 24 Mar 2005. A similar analysis using a single, neighboring radar (Abbeville) is performed for a 9-hour event that occurred on 04 Jul 2005.

During the first step, no corrections are made to the Trappes  $Z_H$  data for attenuation effects. Reflectivity values from adjacent radars are compared if  $\rho_{HV}(0) > 0.97$ , difference in height of measurement  $< 500$  m, range to echoes is  $< 150$  km from both radars,  $Z_H$  from both radars  $> 20$  dBZ, and  $Z_H$ -based, estimated attenuation from the nonpolarimetric radar  $< 1$  dB. The latter threshold is intended to minimize variability that can result due to possible attenuation effects on the neighboring radars.

The gray dotted lines in Fig. 4a-d show normalized densities and mean reflectivity differences between Trappes and its neighboring radars plotted as a function of  $\Phi_{DP}$ . Radar calibration differences between radars were removed by finding mean  $Z_H$  differences at  $\Phi_{DP} < 5^\circ$  (where attenuation effects are minimal) and eliminating the bias from the rest of the measurements. The trends of all mean curves without attenuation correction (solid gray lines) indicate  $Z_H$  measured by Trappes is reduced with increasing  $\Phi_{DP}$ . The reduction is approximately linear in Figs. 4a-c, but appears more nonlinear in Fig. 4d. These comparisons are useful as they may be used for independent evaluation of the advection-correction scheme.

#### b. Correction for attenuation

Next,  $A_h$  and  $A_{hv}$  are retrieved using the advection-correction technique and are used to correct observations of  $Z_H$  and  $Z_{DR}$  based on  $\Phi_{DP}$  measurements. Each retrieval and subsequent correction is event specific. In other words, polarimetric data from Trappes alone are used to produce the lines in Fig. 3. These lines enable us to retrospectively correct  $Z_H$  and  $Z_{DR}$  for attenuation effects. Independent comparisons of  $Z_H$  from Trappes with neighboring radars are once again carried out, and are shown as solid black lines in Fig. 4a-d.

Variability may result in radar-radar comparisons due to a) differing beam propagation paths, b) possible attenuation effects on the neighboring radars, c) slight timing differences at which the data are collected, and d) beam broadening effects. Each case, however, indicates that mean biases in  $Z_H$  have been

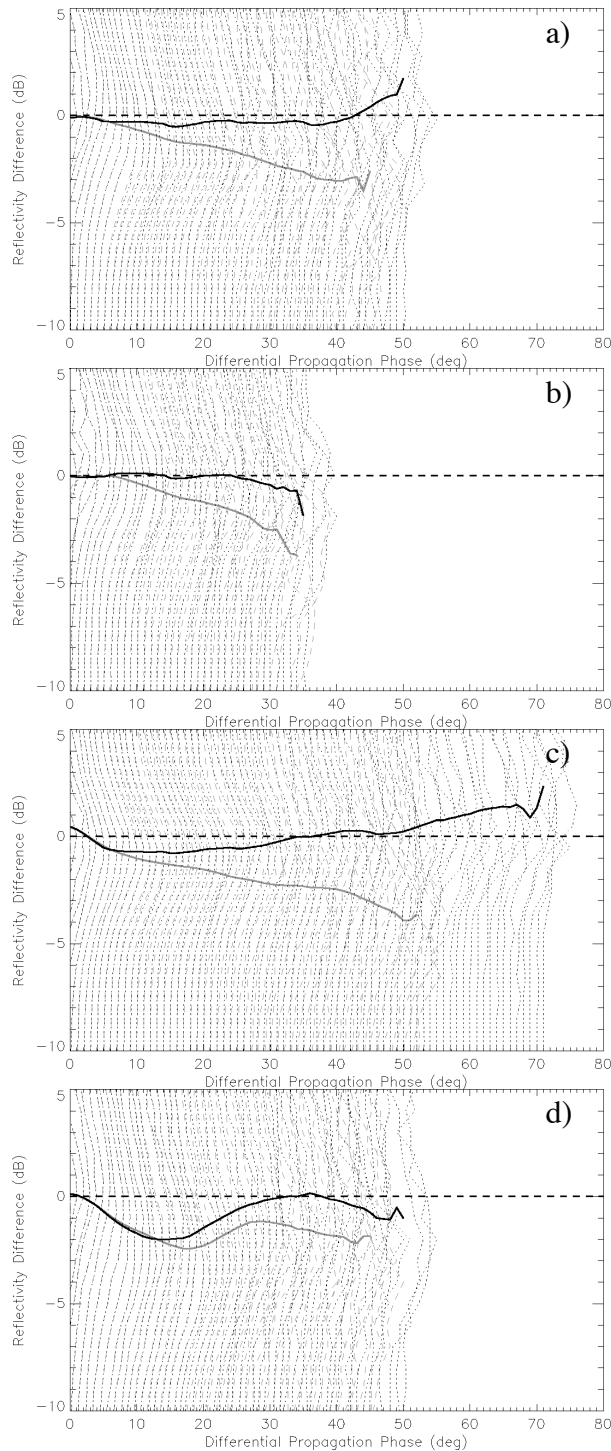


**FIG. 4. Normalized densities (dotted lines) of differences in measured  $Z_H$  between Trappes minus a) Abbeville, b) Bourges, c) Falaise for 24 Mar 2005 case, and d) Abbeville for 04 Jul 2005 case. Solid lines are average differences of comparisons with no attenuation correction applied to Trappes data (in gray), and for corrected data (in black).**

significantly mitigated due to the attenuation correction scheme. The abrupt changes in the curves at high values of  $\Phi_{DP}$  are likely due to smaller sample sizes. It is also noted in Figs. 4c-d that biases as large as  $-2$  dB persist after correction for  $\Phi_{DP}$  values between  $5-20^\circ$ . The corrected curves essentially overlap the uncorrected ones for  $\Phi_{DP}$  values between  $0-10^\circ$ , which is where we would expect attenuation effects to be minimal. This apparent nonlinearity is not fully understood at this time but may be a result of enhanced attenuation due to the so-called “big drop effect” (Carey et al. 2000). Future work will elucidate these comparisons further by analyzing distributions of  $Z_{DR}$  as a function of  $\Phi_{DP}$ . In addition, it is feasible that the raindrop temperatures were anomalously colder at these low  $\Phi_{DP}$  values, which may have also led to enhanced attenuation effects. Temperature distributions as a function of  $\Phi_{DP}$  will also be instrumental in determining if the  $A_h$  and  $A_{hv}$  retrievals need to be dependent on raindrop temperature.

#### 4. CONCLUSIONS

A semi-empirical attenuation correction scheme has been developed using polarimetric radar measurements at C-band. The advection-correction technique is based on the notion that changes in  $Z_H$  and  $Z_{DR}$  following cells over a 5-min time span are due to attenuation effects alone and are related to polarimetric measurements of  $\Phi_{DP}$ . Forecast and observed  $Z_H$  and  $Z_{DR}$  are grouped with their associated changes in  $\Phi_{DP}$ . The attenuation and differential attenuation vectors are then solved for through the minimization of a cost function in a least squares sense. The efficacy of the retrieved horizontal attenuation vectors is examined through independent radar reflectivity comparisons with neighboring radars. Results indicate that this approach mitigates biases in  $Z_H$  due to attenuation.

#### 5. FUTURE WORK

It is noted in two of the cases that the uncorrected reflectivity differences exhibit a slight nonlinear behavior as a function of  $\Phi_{DP}$ . Since linearity is assumed between  $A_h$  and  $\Phi_{DP}$  in the current version of the scheme, the corrected reflectivity differences also show this nonlinearity. Future work will determine if the path-integrated measurements collected in these regions have anomalous values of raindrop temperature and/or  $Z_{DR}$ . Further enhancements in the scheme may be realized once raindrop temperature and “big drop effects” are taken into consideration.

#### 6. ACKNOWLEDGEMENTS

This work was done in the frame of the PANTHERE Project (Programme Aramis Nouvelles Technologies en Hydrometeorologie Extension et REouvellement supported by Meteo-France, the French “Ministere de L’Ecologie et du Developpement

Durable”, the “European Regional Development Fund (ERDF)” of the European Union and CEMAGREF.

## 7. REFERENCES

- Bringi, V. N., V. Chandrasekar, N. Balakrishnan, and D. S. Zrníc, 1990: An examination of propagation effects in rainfall on radar measurements at microwave frequencies. *J. Atmos. Oceanic Technol.*, **7**, 829-840.
- Carey, L. D., S. A. Rutledge, D. A. Ahijevych, and T. D. Keenan, 2000: Correcting propagation effects in C-band polarimetric radar observations of tropical convection using differential propagation phase, *J. Appl. Meteor.*, **39**, 1405-1433.
- Holt, A. R., 1988: Extraction of differential propagation phase from data from S-band circularly polarized radar. *Electron. Lett.*, **24**, 1241-1242.
- Ryzhkov, A. V., and D. S. Zrníc, 1995: Precipitation and attenuation measurements at a 10-cm wavelength. *J. Appl. Meteor.*, **34**, 2121-2134.